Bond order potentials: a study of s- and sp-valent systems

1993 J. Phys.: Condens. Matter 5 5795

(http://iopscience.iop.org/0953-8984/5/32/010)

J. Phys.: Condens. Matter 5 (1993) 5795–5810. Printed in the UK

Bond order potentials: a study of s- and sp-valent systems

P Alinaghian†, P Gumbsch†¶, A J Skinner‡ and D G Pettifor§

† Department of Mathematics, Imperial College of Science, Technology and Medicine, London SW7 2BZ, UK

‡ Complex Systems Theory Branch, Naval Research Laboratory, Washington DC 20375-5000, USA

§ Department of Materials, University of Oxford, Parks Road, Oxford OX1 3PH, UK

Received 1 June 1993

Abstract. The relative structural stability of s- and sp-valent systems is examined within the fourth-moment approximation to the recently derived tight binding bond order potentials. At this low level of approximation we find that the application of a sum rule constraint to the choice of terminator is necessary to get good results. In particular, the competition between graphite, diamond and simple cubic sp-valent lattices is modelled well by the new angularly dependent bond order potentials.

1. Introduction

Atomistic modelling has become an important and increasingly popular tool in modern materials science (Vitek and Srolovitz 1989, Daw and Schlüter 1990) . However, atomistic modelling relies on the availability of simple, yet realistic interatomic potentials. In the last few years we have seen rapid progress in the development of semi-empirical many-body potentials, the simplest of which are the embedded atom potentials (Daw and Baskes 1984, Finnis and Sinclair 1984). Embedded atom potentials are applicable to simple metals and noble metals, but have had only limited success in describing the BCC transition metals and fail to describe the bonding in semiconductors. The modelling of the open structures of semiconductors requires the inclusion of explicit three-body terms (Stillinger and Weber 1985, Tersoff 1988, Baskes *et al* 1989), the forms of which have usually been chosen empirically and fitted to some bulk and cluster properties.

In contrast, the recently proposed bond order potentials, which will be introduced in more detail below, allow us to *derive* the form and angular character of the potentials from tight binding (TB) Hückel theory (Pettifor 1989, Pettifor 1990). The bond order potentials are based on the embedding of a bond (rather than an atom) in its environment and can be expressed as an exact many-atom expansion (Aoki and Pettifor 1993). Bond order potentials therefore seem capable of describing not just a small section of the periodic table, but the whole range of covalently bonded sp- and sd-valent systems.

In this paper we study the properties of the bond order potentials for s- and sp-valent systems. In section 2 we introduce the concept of the bond order and show in section 3 that it may be expressed as an exact many-atom expansion. In section 4 we present a recently derived sum rule, which gives us an explicit criterion for the termination of the many-atom

¶ Present address: Max-Planck-Institut für Metallforschung, Institut für Werkstoffwissenschaft, Seestrasse 92, 70174 Stuttgart, Federal Republic of Germany.

0953-8984/93/325795+16$07.50

expansion. In sections 5 and 6 we compare the relative structural stability of some s- and sp-bonded systems within the symmetric fourth moment approximation (SFMA). In section 7 we conclude.

2. The bond order

Within the tight binding bond model (Sutton *et al* 1988) the total binding energy per atom for a sp-valent system is written as

$$U_{\text{tot}} = U_{\text{rep}} + U_{\text{prom}} + U_{\text{bond}} \tag{1}$$

where U_{rep} is a semi-empirical pairwise repulsive contribution, U_{prom} is the promotion energy which represents the energy penalty incurred in changing the s- and p-occupancy on band formation, and U_{bond} is the covalent bond energy. The bond energy results from evaluating the local density of states $n^{i\alpha}(E)$ associated with orbital α on site i within the two-centre, orthogonal TB approximation:

$$U_{\text{bond}} = \sum_{i\alpha} 2\,\mathcal{N}^{-1} \int^{E_F} (E - E^{i\alpha}) n^{i\alpha}(E)\,\mathrm{d}E \tag{2}$$

where $\mathcal{N}$ is the number of atoms in the system, $E^{i\alpha}$ is the energy level of orbital α on site i and E_F is the Fermi energy. The prefactor 2 accounts for the spin degeneracy in the non-magnetic systems considered in this paper. We usually refer to (2) as the *central-site* description of the bond energy. (The importance of using the *bond* energy rather than the *band* energy within semi-empirical schemes is discussed in detail by Pettifor (1990).) Alternatively, using the definition of the Greenian

$$(E - H)G = 1 \tag{3}$$

and defining the Green function as the matrix element of the Greenian with respect to atomic orbitals $|i\alpha\rangle$ ($\alpha = s, z, x, y$), we have

$$(E - E^{i\alpha})G^{i\alpha i\alpha} = 1 + \sum_{j\beta, j\neq i} H^{i\alpha j\beta} G^{j\beta i\alpha}. \tag{4}$$

Hence, identifying the imaginary part of the Green function with the density of states, we can rewrite (2) in terms of the individual bond energies (Sutton *et al* 1988, Finnis *et al* 1988), namely

$$U_{\text{bond}} = \frac{1}{2}\mathcal{N}^{-1} \sum_{i,j} U^{ij}_{\text{bond}} = \sum_{i\alpha j\beta, i\neq j} 2\,\mathcal{N}^{-1} H^{i\alpha j\beta} \Im \int^{E_F} G^{j\beta i\alpha}\,\mathrm{d}E \tag{5}$$

that is

$$U_{\text{bond}} = \frac{1}{2}\mathcal{N}^{-1} \sum_{i\alpha j\beta, i\neq j} 2H^{i\alpha j\beta} \Theta^{j\beta i\alpha} \tag{6}$$

where $\Im$ stands for the imaginary part and $G^{j\beta i\alpha} = \langle j\beta|(E - H)^{-1}|i\alpha\rangle$.

The *inter-site* description of the bond energy (6), is particularly transparent. It describes the covalent bond energy between a given pair of atoms i and j as the product of the Slater and Koster (1954) two centre energy integral matrix elements $H^{i\alpha j\beta} = \langle i\alpha|H|j\beta\rangle$ and the bond order matrix $\Theta^{j\beta i\alpha}$. The bond order itself gives the difference $(N^+ - N^-)$ between the number of electrons projected onto the bonding $\frac{1}{\sqrt{2}}|i\alpha + j\beta\rangle$ and anti-bonding $\frac{1}{\sqrt{2}}|i\alpha - j\beta\rangle$ states. We note that with this definition of bonding / anti-bonding states the p_z orbitals on

sites i and j must be taken as $|iz\rangle$ and $-|jz\rangle$, respectively when the z axis is along R_{ij}. The matrix $H^{i\alpha j\beta}$ is then symmetric. Although (6) gives the bond energy in terms of individual pairs of atoms, it is important to realize that it is not pairwise since the bond order itself depends upon the local many-atom environment.

Part of the sum in (6) is a trace with respect to the orbital indices (α, β). This can be simplified by changing the basis through a unitary transformation which diagonalizes $H^{i\alpha j\beta}$. Assuming that the spσ bond integral is describable by the geometric mean of $|ss\sigma|$ and ppσ, the 2×2 σ block of the intersite Hamiltonian may be diagonalized with diagonal elements of $-(|ss\sigma| + pp\sigma)$ and zero, respectively (Pettifor 1990). The corresponding hybrid basis function associated with atom i are

$$|i\sigma\rangle = \left(\sqrt{|ss\sigma|}\,|is\rangle + \sqrt{pp\sigma}\,|iz\rangle\right)/\sqrt{|ss\sigma| + pp\sigma} \tag{7}$$

and

$$|i\sigma_0\rangle = \left(\sqrt{pp\sigma}\,|is\rangle - \sqrt{|ss\sigma|}\,|iz\rangle\right)/\sqrt{|ss\sigma| + pp\sigma} \tag{8}$$

whereas the basis function for atom j are

$$|j\sigma\rangle = \left(\sqrt{|ss\sigma|}\,|js\rangle - \sqrt{pp\sigma}\,|jz\rangle\right)/\sqrt{|ss\sigma| + pp\sigma} \tag{9}$$

and

$$|j\sigma_0\rangle = \left(\sqrt{pp\sigma}\,|js\rangle + \sqrt{|ss\sigma|}\,|jz\rangle\right)/\sqrt{|ss\sigma| + pp\sigma}. \tag{10}$$

We see that

$$\langle i\sigma|H|j\sigma\rangle = -(|ss\sigma| + pp\sigma) \tag{11}$$

$$\langle i\sigma_0|H|j\sigma_0\rangle = 0 \tag{12}$$

and the off diagonal matrix elements vanish. Equation (6) therefore reduces to the following simple form (Pettifor and Aoki 1992)

$$U^{ij}_{\text{bond}} = -2(|ss\sigma| + pp\sigma)_{ij}\Theta^{j\sigma i\sigma} - 4(pp\pi)_{ij}\Theta^{j\pi i\pi} \tag{13}$$

where $\Theta^{j\sigma i\sigma}$ is the bond order between hybrid orbitals $|i\sigma\rangle$ and $|j\sigma\rangle$. The bond order for the π bond is given by $\Theta^{j\pi i\pi} = (1/2)(\Theta^{jxix} + \Theta^{jyiy})$.

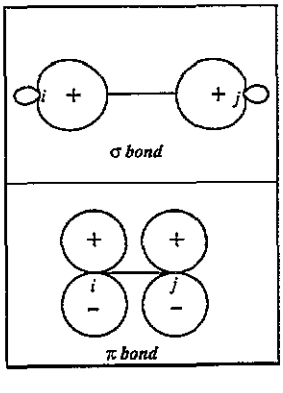

Figure 1. The σ and π orbitals for two sp-valent atoms i and j.

Figure 1 displays schematically the σ and π orbitals for two sp-valent atoms i and j. The σ orbitals can be thought of as a generalization of the familiar sp^3-hybrid orbital to which they reduce for the special case of $p_\sigma = pp\sigma/|ss\sigma| = 3$. We note that the above hybrid orbitals are independent of the environment about the bond. For $sp\sigma = \sqrt{|ss\sigma|pp\sigma}$ they represent an exact transformation of (6) into the more transparent form of (13).

The bond order, which is given by the difference between the number of electrons in bonding and anti-bonding states, can be written as

$$\Theta^{ij}(E_F) = N^+ - N^- = -\frac{1}{\pi}\Im\int^{E_F}[G^+_{00}(E) - G^-_{00}(E)]\,dE \tag{14}$$

where for simplicity the orbital labels have been left out. The bonding and anti-bonding Green functions can be written as a continued fraction (Haydock *et al* 1972, Haydock 1980), namely

$$G^\pm_{00}(E) = \langle u^\pm_0|(E-H)^{-1}|u^\pm_0\rangle = \cfrac{1}{E - a^\pm_0 - \cfrac{(b^\pm_1)^2}{E - a^\pm_1 - \cfrac{(b^\pm_2)^2}{E - a^\pm_2 - \ldots}}} \tag{15}$$

where $|u^\pm_0\rangle = \frac{1}{\sqrt{2}}|i\alpha \pm j\beta\rangle$. The coefficients are determined by the Lanczos algorithm, namely

$$b^\pm_{n+1}|u^\pm_{n+1}\rangle = H|u^\pm_n\rangle - a^\pm_n|u^\pm_n\rangle - b^\pm_n|u^\pm_{n-1}\rangle \tag{16}$$

with the boundary condition that $|u^\pm_{-1}\rangle = 0$. The dependence of the recursion coefficients on the local atomic environment about the bond ij can be found by using the well known relationship between the recursion coefficients and the moments (see for example Pettifor and Aoki (1991), equations (2.10)–(2.15)).

3. The many atom expansion

Recently Aoki and Pettifor (1993) have shown that the bond order can be written as an *exact* many-atom expansion. They considered acting with the Lanczos algorithm on the starting orbital $|u^\lambda_0\rangle = (|i\rangle + e^{i\theta}|j\rangle)/\sqrt{2}$ where $\theta = \cos^{-1}\lambda$. The corresponding Green function

$$G^\lambda_{00}(E) = \langle u^\lambda_0|(E-H)^{-1}|u^\lambda_0\rangle = G^0_{00}(E) + \lambda G^{ij}(E) \tag{17}$$

can, therefore, be written as a continued fraction like (15) with recursion coefficients a^λ_n and b^λ_n. It follows from (17) that G^λ_{00} is *linear* with respect to λ so that

$$G^{ij}(E) = \left(\frac{dG_{00}}{d\lambda}\right)_0 = \sum_{n=0}^{\infty}\left(\frac{\partial G^\lambda_{00}}{\partial a^\lambda_n}\right)_0 \delta a_n + \sum_{n=1}^{\infty}\left(\frac{\partial G^\lambda_{00}}{\partial b^\lambda_n}\right)_0 \delta b_n \tag{18}$$

where

$$\delta a_n = (da^\lambda_n/d\lambda)_0 \qquad \text{and} \qquad \delta b_n = (db^\lambda_n/d\lambda)_0 \tag{19}$$

with $(\ldots)_0$ denoting $\lambda = 0$.

In this paper we will consider only those structures which have even-membered rings so that all odd moments vanish provided we take the sp energy separation E_{sp} to be zero. This implies that $\delta b_n = 0$ (see equations (22)–(25) of Aoki and Pettifor 1993). Substituting (18) in (5) and keeping only sufficient terms in the expansion to guarantee up to the correct

fourth-moment μ_4 (cf section 3.2 of Aoki *et al* 1993a), the bond order for a particular bond is given by

$$\Theta(E_F) = -2\left\{\chi_2(E_F)\zeta_2 + \chi_4(E_F)[\zeta_4^{\text{ring}} - \zeta_2^3/(b_1^0)^2]\right\} \tag{20}$$

where the response functions $\chi_{2n+2}(E_F)$ are defined by

$$\chi_{2n+2}(E_F) = \frac{1}{\pi}\Im\int^{E_F} G_{0n}(E)G_{n0}(E)\,\mathrm{d}E \tag{21}$$

and $\zeta_2 = \delta a_0$ and $(\zeta_4^{\text{ring}} - \zeta_2^3)/(b_1^0)^2 = \delta a_1$. Analytic expressions for χ_2 and χ_4 are given in the appendix within the SFMA. ζ_2 corresponds to the appropriate bond integral $\langle i\alpha|H|j\alpha\rangle$ and ζ_4^{ring} is the corresponding four-atom ring contribution which for sp-valent systems has been given explicity by equations (50) and (52) of Pettifor and Aoki (1992). The coefficient b_1^0 equals $b_1^{\lambda=0}$ and is given by the average second moment about sites i and j, namely

$$(b_1^0)^2 = \mu_2 = \tfrac{1}{2}[\langle i|H^2|i\rangle + \langle j|H^2|j\rangle]. \tag{22}$$

4. A sum rule

The truncation of the many-atom expansion after just the first few terms may result in the violation of (4) which gives the relation between the *on-site* Green function $G^{i\alpha i\alpha}$ and *intersite* Green functions $G^{j\beta i\alpha}$. On making the above truncation, therefore, we will constrain our choice of terminator (represented by the unknown coefficients a_∞ and b_∞ in the square root terminator that enters in the response functions in the appendix) so that the identity is maintained for the particular choice of energy $E = E^{i\alpha}$ (Aoki *et al* 1993a, b), namely

$$1 + \sum_{j\beta, j\neq i} H^{i\alpha j\beta}G^{j\beta i\alpha}(E^{i\alpha} + \mathrm{i}0) = 0. \tag{23}$$

This guarantees that the number of electrons $N^{i\alpha}$ is calculated consistently within the approximations made. By taking the imaginary part of (4) we find that the local density of states for an orbital on atom i can be expressed in terms of the intersite Green functions as

$$n^{i\alpha}(E) = (E - E^{i\alpha})^{-1}\left(\frac{-1}{\pi}\right)\sum_{j\beta, j\neq i} H^{i\alpha j\beta}\Im G^{j\beta i\alpha}(E + \mathrm{i}0) \qquad (E \neq E^{i\alpha}). \tag{24}$$

Here we see that the condition

$$\sum_{j\beta, j\neq i} H^{i\alpha j\beta}\Im G^{j\beta i\alpha}(E^{i\alpha} + \mathrm{i}0) = 0 \tag{25}$$

must be fulfilled in order to avoid an unphysical singularity in $n^{i\alpha}(E)$ at $E = E^{i\alpha}$ which would bring a logarithmic singularity in the number of electrons $N^{i\alpha}$ as a function of the Fermi level E_F. Equation (25) constitutes the imaginary part of (23). Since the integration of $n^{i\alpha}(E)$ up to infinity must give unity, namely

$$1 = \sum_{j\beta, j\neq i} H^{i\alpha j\beta}\left(\frac{-1}{\pi}\right)\mathrm{P}\int_{-\infty}^{\infty}\frac{\Im G^{j\beta i\alpha}(E + \mathrm{i}0)}{E - E^{i\alpha}}\,\mathrm{d}E \tag{26}$$

we find a sum rule using the Kramers–Kronig relation as

$$1 + \sum_{j\beta, j\neq i} H^{i\alpha j\beta}\Re G^{j\beta i\alpha}(E^{i\alpha} + \mathrm{i}0) = 0 \tag{27}$$

where $\Re$ stands for the real part and this constitutes the real part of (23).

If we assume that the atomic energy levels are orbital independent (corresponding to $E_{sp} = 0$), then we find from a similar argument with respect to the total number of electrons on atom i that the sum rule may be written

$$\sum_{\alpha} 1 + \sum_{j\alpha\beta, j\neq i} H^{i\alpha j\beta} G^{j\beta i\alpha}(\mathrm{i}0) = 0 \tag{28}$$

where $E^{i\alpha}$ has been taken as the energy zero. It should be noted that this formula is invariant under the rotation of the quantization axes (or unitary transformation) for local orbitals α and β on each pair of atoms i and j. Therefore, choosing the orbitals such that $H^{i\alpha j\beta}$ is diagonalized, the sum rule takes the form of

$$\sum_{\alpha} 1 + \sum_{j\alpha, j\neq i} H^{i\alpha j\alpha} G^{j\alpha i\alpha}(\mathrm{i}0) = 0. \tag{29}$$

By taking the real and imaginary part of (29) we can make use of this sum rule to fix the two parameters a_∞ and b_∞ in the square root terminator to the approximate intersite Green functions.

For a system of identical s-valent atoms, the sum rule simplifies to

$$1 + \sum_{j\neq i} H^{ij} G^{ij}(\mathrm{i}0) = 0 \tag{30}$$

For structures with no odd-member rings the truncated intersite Green function automatically fulfils the imaginary part of the sum rule (30) as $\Im G^{ij}(\mathrm{i}0) = 0$ by symmetry of the bonding and anti-bonding density of states; only the real part remains to be fulfilled.

5. s-valent systems

In this section we use the sum rule to study simple s-bonded structures with even membered rings only. We use the square root terminator with $b_2^0 = b_3^0 = \ldots = b_\infty$. Substitution of (18) into the sum rule (27) requires the following terms:

$$\Re[G_{00}(0)G_{00}(0)] = -b_\infty^2/(b_1^0)^4 \tag{31}$$

$$\Re[G_{00}(0)G_{10}(0)] = 0 \tag{32}$$

$$\Re[G_{01}(0)G_{10}(0)] = 1/(b_1^0)^2 \tag{33}$$

which have been evaluated using some simple algebra within the SFMA (Aoki *et al* 1993b). The sum rule, therefore, takes the form

$$1 = \sum_{j\neq i} H^{ij} \left\{ b_\infty^2 - \left[\frac{\zeta_4^{\mathrm{ring}}}{\zeta_2} - \zeta_2^2 \right] \right\} \frac{\zeta_2}{(b_1^0)^4} \tag{34}$$

where the individual terms inside the sum are dependent on the particular bond ij. For the case of s orbitals on a lattice where all sites are equivalent (34) is satisfied for

$$b_\infty^2 = \frac{\zeta_4^{\mathrm{ring}} - \zeta_2^3}{\zeta_2} + (b_1^0)^2. \tag{35}$$

The right-hand side of this equation, however, is simply $(b_2^0)^2$ where b_2^0 is the recursion coefficient $b_2^{\lambda=0}$ which may be defined (Pettifor and Aoki 1991) in terms of the *exact* average second and fourth moments, namely

$$(b_2^0)^2 = (\mu_4 - \mu_2^2)/\mu_2 = \frac{\zeta_4^{\mathrm{ring}} - \zeta_2^3}{\zeta_2} + (b_1^0)^2. \tag{36}$$

Thus the sum rule implies that we must choose our terminator so that $b_\infty = b_2^0$ where b_2^0 is the exact recursion coefficient $b_2^{\lambda=0}$. At this fourth-moment level of approximation we include in the average Green function information about the shape of the band, because $(b_2^0/b_1^0)^2$ is a measure of the ratio of the fourth and the second moments of the density of states. As $(b_2^0/b_1^0)^2$ becomes larger than unity the band develops a distinct maximum at its centre. If b_2^0 equals b_1^0 we have a semi-elliptic band and as $(b_2^0/b_1^0)^2$ becomes smaller than unity a pseudo-gap develops in the centre of the band and increasingly more weight is pushed towards the band edges. At $(b_2^0/b_1^0)^2 = \frac{1}{2}$ the band has a singularity at the band edge and below this value δ-functions occur outside the continuum band of states. In the most extreme case, when b_2^0 vanishes, as for the dimer, the continuum band of states vanishes and we are left with the two δ-functions.

We now apply the bond order potentials to study a few simple s-bonded structures with only even membered rings. The structures we investigate are: the dimer, the linear chain, the diamond lattice, the two-dimensional square lattice, the simple cubic lattice and the BCC lattice. Within the fourth-moment approximation and with only nearest-neighbour hopping it follows from equations (6) and (20) that the normalized bond energy per atom for the above s-valent lattices can be written

$$U^{\text{bond}}/b_1^0 = \left\{\hat{\chi}_2(b_2^0/b_1^0, N_\sigma) + \hat{\chi}_4(b_2^0/b_1^0, N_\sigma)[(b_2^0/b_1^0)^2 - 1]\right\}. \tag{37}$$

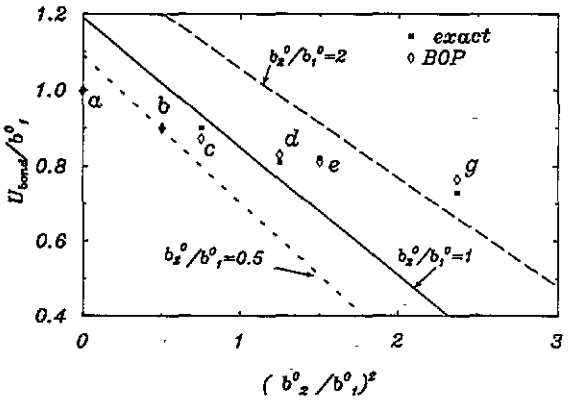

Figure 2. The normalized bond energy versus the normalized fourth moment for different approximations within the s-valent bond order potentials for a half-full band. The dotted, solid and dashed lines correspond to evaluating the normalized response functions with the constant value of $b_2^0/b_1^0 = 0.5$, 1 and 2, respectively whereas the open diamonds use the correct structure dependent value of b_2^0/b_1^0. The solid squares give the exact TB results from Brown and Carlsson (1985). In this and the following figure the letters indicate the structure: (a) dimer, (b) linear chain, (c) diamond structure, (d) two-dimensional square lattice, (e) simple cubic structure and (g) body-centred cubic lattice.

The reduced susceptibilities $\hat{\chi}_{2n+2} = |b_2^0|\chi_{2n+2}$ are functions only of (b_2^0/b_1^0) and the fractional occupancy of the band N_σ, since the terminator b_∞ has been chosen equal to b_2^0 in order to satisfy the sum rule, (30). Note that $(b_1^0)^2 = \mu_2$ and $(b_2^0/b_1^0)^2 = \mu_4/\mu_2^2 - 1$ from equations (22) and (36). Figure 2 displays the dependence of the normalized bond energy per atom U^{bond}/b_1^0 on the normalized fourth moment $(b_2^0/b_1^0)^2$ for the case of a half-full band with $N_\sigma = 0.5$. Such a figure was first constructed by Brown and Carlsson (1985) whose exact values for the TB bond energies for the different lattices are indicated by the solid

squares. The three lines in figure 2 show the linear dependence to be expected from (37) if the *reduced* susceptibilities are assumed to be structure independent by taking $\hat{\chi}_2$ and $\hat{\chi}_4$ as constants. The particular choices $(b_2^0/b_1^0)^2 = 0.5$, 1.0 and 2.0 have been plotted. Using the correct values of b_2^0/b_1^0 in the response functions (the diamond symbols in figure 2) gives excellent bond energies for the different structures considered. Moreover, we find that truncating the *intersite* many-atom expansion at the fourth moment and using the sum rule to fix b_∞ gives the same results as the *central site* method taken to the fourth-moment level of Brown and Carlson (1985) (Aoki *et al* 1993b). Within the SFMA the *exact* TB results are obtained for the diatomic molecule and the linear chain. Figure 3 demonstrates that this convergence of the bond order potential (BOP) expansion is equally good for band fillings away from half-full, notably $N_\sigma = 0.1$, 0.2 and 0.3.

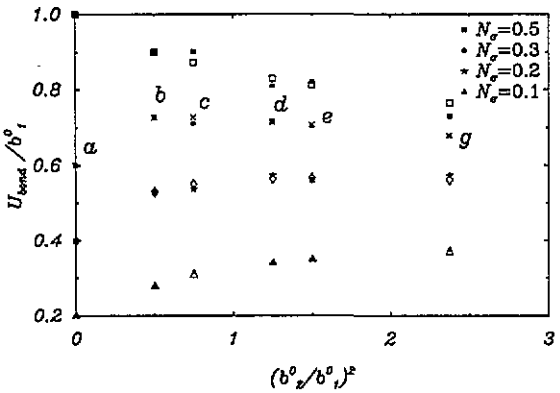

Figure 3. The normalized bond energy versus the normalized fourth-moment for different band fillings for s-valent systems. The exact TB results are taken from Brown and Carlsson (1985).

Finally, we have studied the behaviour of the BOP as compared to the central-site recursion method with respect to defect formation. We do this by evaluating the formation energies for the creation of a vacancy or a surface in some of the structures analysed above. The bond energy contribution to the formation energy is defined as the difference between the bond energy of the defected structure and the bond energy of a perfect structure with the same number of atoms. Figure 4 shows the bond energy contributions to the defect formation energies normalized by the magnitude of the nearest-neighbour hopping integral h for a half-full band and for a band filling of $N_\sigma = 0.3$. The very satisfactory agreement between the two methods is also found for other band fillings.

6. sp-valent systems

In this section we study the structural stability of sp-valent systems with respect to the simple cubic, diamond and two-dimensional graphite structures. All these structures have no odd member rings which implies that the density of states is symmetric if we assume zero sp splitting, namely $E_{sp} = 0$.

The choice of the coefficients in the terminator is determined by the sum rule as follows. Since the σ and π bands have the same width we take $b_\infty^{0,\sigma} = b_\infty^{0,\pi} = b_\infty$. Keeping only $b_1^{0,\sigma}$ and $b_1^{0,\pi}$ in the response functions and choosing all remaining recursion coefficients

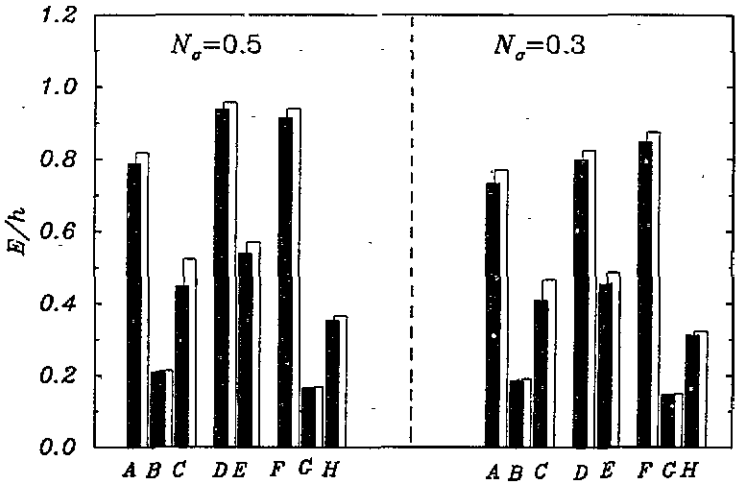

Figure 4. The normalized defect energies of s-valent systems with h=−ssσ as calculated from the BOP (solid rectangles) and from the central site recursion method (open rectangles) for different band fillings. The letters indicate the following defects: A the vacancy, B the (10) surface and C the (11) surface in the two-dimensional square lattice; D the vacancy and E the (100) surface in the diamond structure; F the vacancy, G the (100) surface and H the (110) surface in the simple cubic structure.

equal to b_∞ would lead to a value of b_∞ much smaller than $b_1^{0,\sigma}$ and $b_1^{0,\pi}$ when the sum rule is applied. This gives non-physical delta functions outside the band edges. Therefore, in order to avoid this we have chosen the square root terminator through $b_2^{0,\sigma} = b_2^{0,\pi} = \tilde{b}_2$ and $b_3^{0,\sigma} = b_3^{0,\pi} = b_4^{0,\sigma} = b_4^{0,\pi} = \cdots = b_\infty$ where b_∞ takes the form (Aoki 1993)

$$b_\infty^2 = (\tilde{b}_1^2 + \tilde{b}_2^2)/2. \tag{38}$$

The average $\tilde{b}_1$ is chosen as that value of b_∞ which satisfies the sum rule if the many-atom expansion is truncated after the first term and the response function χ_2 has all recursion coefficients equal. It is given by

$$\tilde{b}_1^2 = (4/z)/\left[(\zeta_2^\sigma)^2/(b_1^{0,\sigma})^4 + 2(\zeta_2^\pi)^2/(b_1^{0,\pi})^4\right] \tag{39}$$

where z is the nearest neighbours or coordination number. $\tilde{b}_2$ is then found by satisfying the sum rule within the SFMA, namely

$$2\tilde{b}_2^4\left\{\frac{(\zeta_2^\sigma)^2}{(b_1^\sigma)^4} + 2\frac{(\zeta_2^\pi)^2}{(b_1^\pi)^4}\right\} - \left\{\frac{4}{z} + \frac{\zeta_2^\sigma[\zeta_4^{\mathrm{ring},\sigma} - (\zeta_2^\sigma)^3]}{(b_1^\sigma)^4} + 2\frac{\zeta_2^\pi[\zeta_4^{\mathrm{ring},\pi} - (\zeta_2^\pi)^3]}{(b_1^\pi)^4}\right\}(\tilde{b}_1^2 + \tilde{b}_2^2) = 0. \tag{40}$$

This leads to

$$\tilde{b}_2^2 = (-B + (B^2 - 4AC)^{1/2})/(2A) \tag{41}$$

where

$$A = 2\left[\frac{(\zeta_2^\sigma)^2}{(b_1^{0,\sigma})^4} + 2\frac{(\zeta_2^\pi)^2}{(b_1^{0,\pi})^4}\right] \tag{42}$$

$$B = -\left\{4/z + \frac{\zeta_2^\sigma[\zeta_4^{\mathrm{ring},\sigma} - (\zeta_2^\sigma)^3]}{(b_1^{0,\sigma})^4} + 2\frac{\zeta_2^\pi[\zeta_4^{\mathrm{ring},\pi} - (\zeta_2^\pi)^3]}{(b_1^{0,\pi})^4}\right\} \tag{43}$$

and

$$C = B\tilde{b}_1^2. \tag{44}$$

Therefore, the SFMA requires the calculation of the second moments entering $b_1^{0,\alpha}$ and the evaluation of all four of the four-member rings around a given bond. This calculation is a particularly simple task for diamond and graphite structures since both structures do not have any four-member rings within the nearest-neighbour approximation.

We now compare the results obtained within the SFMA when the sum rule is satisfied, with that when it is not applied, and compare both to more accurate results which we have obtained by retaining 20 exact levels around a given bond in the continued fraction, equation (15). We have taken Chadi's values of $p_\sigma = \text{pp}\sigma/|\text{ss}\sigma| = 1.5738$ and $p_\pi = |\text{pp}\pi|/|\text{ss}\sigma| = 0.5547$ (Chadi 1979). Following Cressoni and Pettifor (1991) the σ and π bond integrals are assumed to display the same functional dependence on interatomic distance, namely

$$\left.\begin{matrix}(|\text{ss}\sigma| + \text{pp}\sigma) \\ \text{pp}\pi\end{matrix}\right\} = \left.\begin{matrix}(1 + p_\sigma) \\ -p_\pi\end{matrix}\right\} h(R_{ij}) \tag{45}$$

where R_{ij} is the distance between the two atoms i and j. For lattices considered here where all neighbour bonds are equal in length the coefficient b_1^0 takes a particularly simple form. For the σ bond between the hybrid orbitals $|i\sigma\rangle$ and $|j\sigma\rangle$ we have (Pettifor 1990)

$$(b_1^{0,\sigma}/\zeta_2^\sigma)^2 = 1 + \sum_{k\neq i,j} g_\sigma(\theta_k) \tag{46}$$

where k is a nearest neighbour to atom i, θ_k is the corresponding bond angle and $\zeta_2^\sigma = -(1 + p_\sigma)h(R_{ij})$. The embedding function is given by

$$g_\sigma(\theta) = (1 + p_\sigma \cos\theta)^2/(1 + p_\sigma)^2 + p_\sigma p_\pi^2 \sin^2\theta/(1 + p_\sigma)^3. \tag{47}$$

Similarly for the non-bonding σ state between the hybrid orbitals $|i\sigma_0\rangle$ and $|j\sigma_0\rangle$ we have

$$(b_1^{0,\sigma_0}/\zeta_2^\sigma)^2 = \sum_{k\neq i,j} g_{\sigma_0}(\theta_k) \tag{48}$$

with

$$g_{\sigma_0}(\theta) = \frac{p_\sigma(1 - \cos\theta)^2}{(1 + p_\sigma)^2} + \frac{p_\pi^2 \sin^2\theta}{(1 + p_\sigma)^3}. \tag{49}$$

For the π bond we have

$$(b_1^{0,\pi}/\zeta_2^\pi)^2 = 1 + \sum_{k\neq i,j} g_\pi(\theta_k) \tag{50}$$

where

$$g_\pi(\theta_j) = \tfrac{1}{2}[(p_\sigma/p^2\pi)(1 + p_\sigma)\sin^2\theta + (1 + \cos^2\theta)] \tag{51}$$

and $\zeta_2^\pi = -p_\pi h(R_{ij})$.

Figure 5 illustrates the angular dependence of the embedding function $g_\sigma(\theta)$ and $g_\pi(\theta)$. The pure s bond corresponds to p_σ=0 and displays no angular dependence. The pure p bond corresponds to vanishing ssσ. We see that $g_\sigma(\theta)$ falls to zero for a bond angle 90° for the case $p_\pi = 0$ since then there will be no coupling to neighbouring atoms at right angles to the bond. The sp hybrid bond displays very small values when θ becomes larger than about 100°. For Chadi's parameters it has a minimum around 130° as expected from the behaviour of the hybrid orbitals, shown in figure 1, which have very little weight in this direction. Therefore graphite and diamond lattices with bond angles of 120° and 109°, respectively

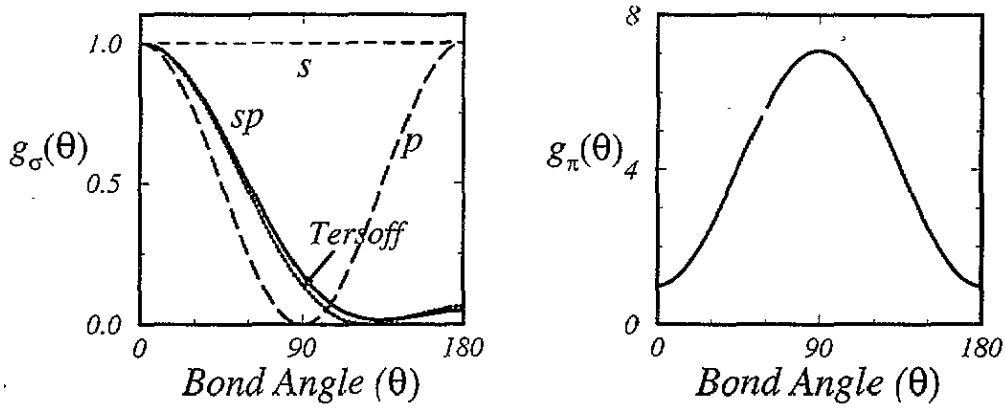

Figure 5. The angular dependence of the embedding functions $g_\sigma(\theta)$ and the $g_\pi(\theta)$. The normalized semi-empirical Tersóff (1988) curve is also shown.

will have nearly *saturated* σ bonds with bond orders close to unity for a half-full band. In contrast the angular dependence of the π bond leads to *unsaturated* behaviour, as can be seen in figure 5, since $g_\pi(\theta)$ rises to a value much larger than that for angularly independent s orbitals. We see that the angular dependence of $g_\sigma(\theta)$ is very similar to that displayed by the semi-empirical potential of Tersoff (1988) (see Pettifor and Aoki 1992). Table 1 gives the normalized sp valent recursion coefficients calculated for the three structures diamond, graphite and simple cubic. The values of $\zeta_4^{\mathrm{ring},\alpha}$ and the ratio of $(\tilde{b}_2/b_1^{0,\alpha})$ are also included. As expected, table 1 shows that the normalized recursion coefficients $b_1^{0,\sigma}/\zeta_2^\sigma$ are very small for the graphite and diamond lattices whereas the normalized $b_1^{0,\pi}/\zeta_2^\pi$ take a large value in all structures.

Table 1. The normalized sp-valent recursion coefficients for the three structures diamond, graphite and simple cubic.

Structure	$b_1^{0,\sigma}/\zeta_2^\sigma$	$\tilde{b}_2/\zeta_2^\sigma$	$\zeta_4^{\mathrm{ring},\sigma}$	$\tilde{b}_2/b_1^{0,\sigma}$
Diamond	1.0854	0.7344	0.00	0.677
Graphite	1.0277	0.7380	0.00	0.718
SC	1.3293	1.2810	$-6.81h^3(R_{ij})$	0.964
Structure	$b_1^{0,\pi}/\zeta_2^\pi$	$\tilde{b}_2/\zeta_2^\pi$	$\zeta_4^{\mathrm{ring},\pi}$	$\tilde{b}_2/b_1^{0,\pi}$
Diamond	4.4966	3.407	0.00	0.758
Graphite	3.4818	3.424	0.00	0.983
SC	5.5072	5.9462	$-6.24h^3(R_{ij})$	1.079
Structure	$b_1^{0,\sigma_0}/\zeta_2^\sigma$	$\tilde{b}_2/\zeta_2^\sigma$	$\zeta_4^{\mathrm{ring},\sigma_0}$	$\tilde{b}_2/b_1^{0,\sigma_0}$
Diamond	1.1468	0.7344	0.00	0.640
Graphite	1.0469	0.7380	0.00	0.705
SC	1.4045	1.2810	$-2.62h^3(R_{ij})$	0.912

Figure 6 illustrates the reduced response functions $\hat{\chi}_2$ and $\hat{\chi}_4$ as a function of the number of electrons per atom in the appropriate σ and π orbitals for the diamond, graphite and simple cubic structures within the SFMA when the sum rule is satisfied.

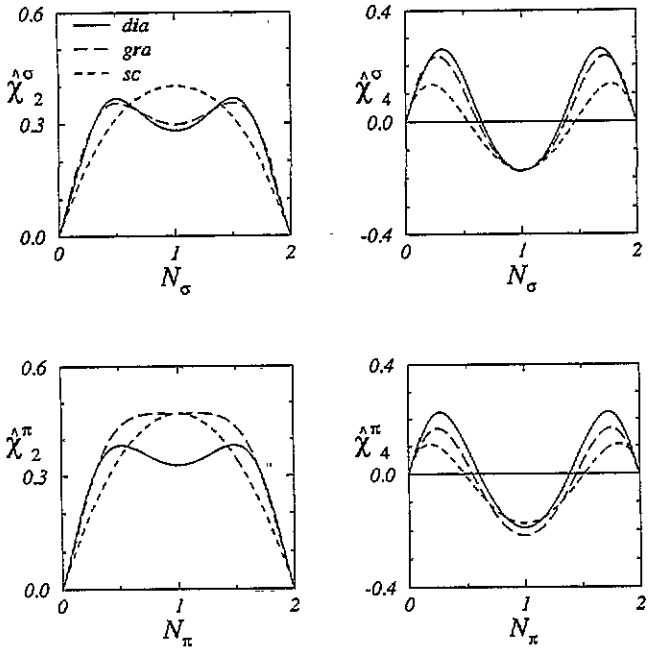

Figure 6. The reduced response functions $\hat{\chi}_2$ and $\hat{\chi}_4$ as a function of the number of electrons per atom in the appropriate σ and π orbitals for the sp-valent diamond, graphite and simple cubic lattices within the SFMA when the sum rule is satisfied.

Figure 7 illustrates the corresponding bond order from (20). The left-hand panels correspond to evaluating the response functions when the sum rule is not applied by using $b_1^{0,\alpha} = b_2^{0,\alpha} = \ldots = b_\infty$, whereas the middle panels correspond to choosing the terminator in order to satisfy the sum rule. The right-hand panels exhibit the results obtained within the intersite method (15), calculated with 20 exact levels about the bond ij. The SFMA predicts a negative σ bond order in small regions at the start and end of the band filling. This is due to the truncation of the many atom expansion. It should be noted that the oscillations in the lower right hand panel for Θ_π for diamond and graphite lattices are probably due to using the simple square root terminator rather than the sophisticated Turchi terminator appropriate for densities of states with a gap (Turchi *et al* 1982) . We see that, as expected, for a half-full band the σ bond order for graphite and diamond is nearly unity whereas that for the π bond is much less than unity.

Figure 8 displays the density of states for diamond, graphite and simple cubic lattices using the integrand in (55) within the SFMA when the sum rule is not applied (left-hand panels) and when the sum rule is satisfied (right-hand panels). The ratio $(\tilde{b}_2/b_1^0)$ determines the shape of the density of states. When this ratio is less than unity, for example in case of the σ bond in the diamond and graphite structure, there is bimodal behaviour. As $(\tilde{b}_2/b_1^0)$ approaches unity the bimodal behaviour disappears, as can be seen for the σ bond in the simple cubic lattice (cf table 1). In the left-hand panels $(\tilde{b}_2/b_1^0) = 1$ for all structures so that all structures have semi-elliptic bands.

The relative structural stability of simple cubic, diamond and graphite lattices was predicted using the structural energy difference theorem (Pettifor 1986). This states that to the first order

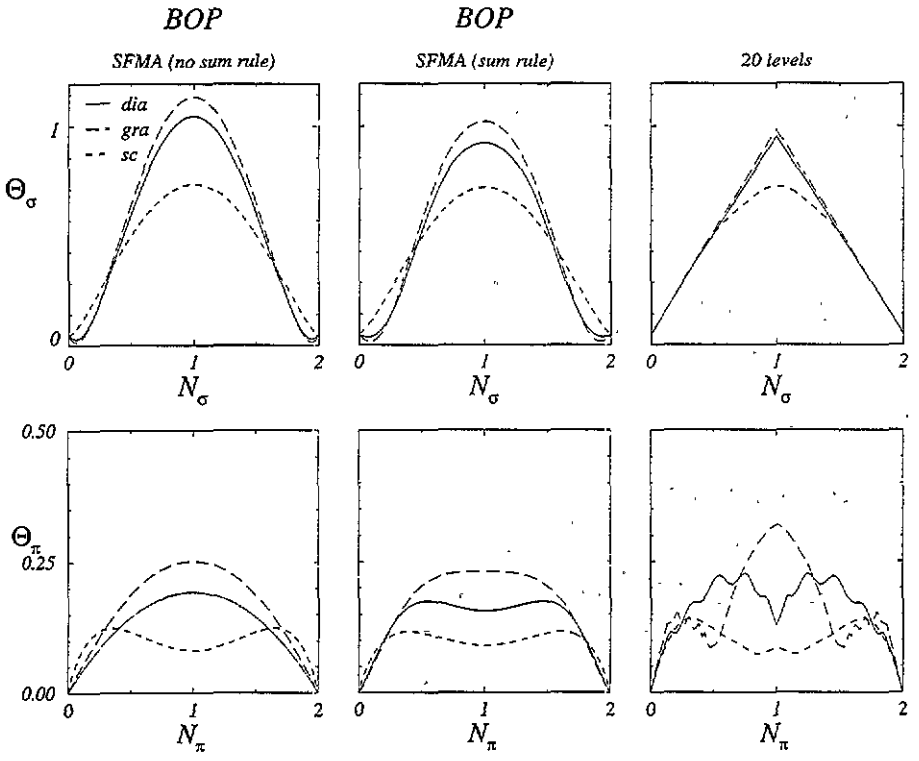

Figure 7. The σ and π bond orders for the sp-valent diamond, graphite and simple cubic lattices. The left-hand panels correspond to evaluating the response functions without the sum rule constraint. The middle panels correspond to choosing the terminator to satisfy the sum rule, and the right hand panels display the results obtained within the intersite method calculated to 20 exact levels about a given bond.

$$\Delta U = [\Delta U_{\text{bond}}]_{\Delta U_{\text{rep}}=0} \tag{52}$$

where $\Delta U_{\text{rep}}=0$ signifies that the bond lengths in each structure have been adjusted so that the change in the repulsive energy from one structure to another is zero. The repulsive energy is taken to be proportional to $h^2(R_{ij})$. This assumption allows us to write $\Delta U = [\Delta U_{\text{bond}}]_{\Delta\mu_2=0}$ where μ_2 is the second moment of the density of states (see Pettifor and Podloucky 1984, Cressoni and Pettifor 1991). Thus we set the second moment of the density of states for each structure to be the same. Within the first nearest-neighbour model this implies that $6h^2(R_{ij})_{\text{sc}} = 4h^2(R_{ij})_{\text{dia}} = 3h^2(R_{ij})_{\text{gra}}$. We take $h(R_{ij})_{\text{sc}} = -\text{ss}\sigma_{\text{sc}} = 1$.

Figure 9 displays the σ and π bond energies as a function of the total number of electrons per atom within the SFMA when sum rule is not applied (left-hand panels) and when it is satisfied (right-hand panels). It can be seen that the σ bond energy is much larger than the π bond energy.

Figure 10 shows the relative structural trends between graphite, diamond and simple cubic lattices within the SFMA when the sum rule is not applied (left-hand panel), when it is satisfied (middle panel) and within the intersite method calculated with 20 exact levels (right-hand panel). All these calculations show the same structural trend, namely, in the half full band region diamond is the most stable structure, whereas with increasing band filling graphite and then simple cubic become more stable. This is to be expected within

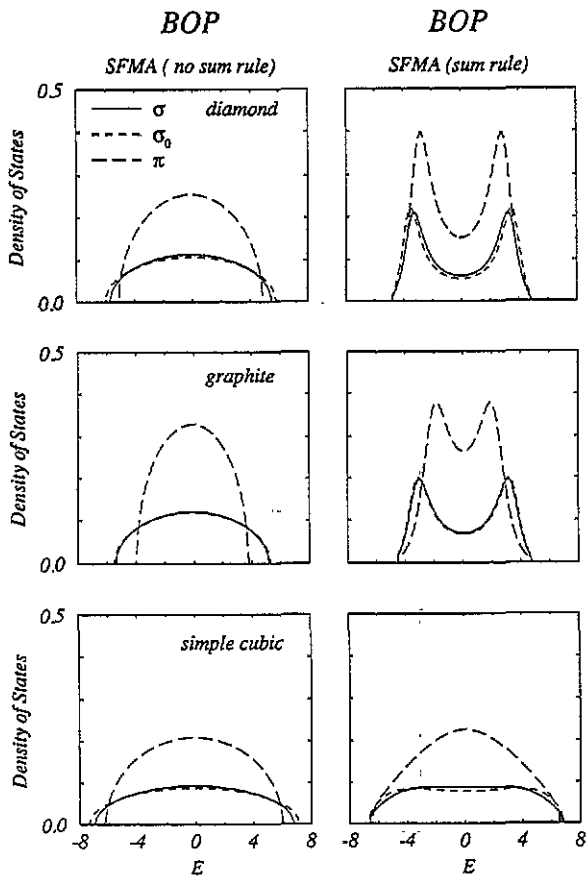

Figure 8. The density of states for diamond, graphite and simple cubic lattices within the SFMA when the sum rule is not applied (the left-hand panels) and when it is satisfied (the right hand panels).

the fourth-moment approximation as has been argued by Cressoni and Pettifor (1991) who also considered other structure types in their detailed comparison of TB predictions with experimental structural trends across the sp-valent elements in the periodic table. We see from figure 10 that for half-full bands the SFMA predicts a band energy that is within 2% of the converged result when the sum rule is satisfied, whereas not applying the sum rule leads to a much poorer result with 13% error.

7. Conclusions

We have examined the relative structural stability of s- and sp-valent lattices using the bond order potentials within the SFMA. We have shown that the results of the SFMA with the sum rule satisfied are comparable with accurate TB results and predict the expected structural trend from simple cubic → graphite → diamond → graphite → simple cubic as a function of the band filling if the relative stability of only these three structure types is considered. We are currently extending these calculations to treating the $E_{sp} \neq 0$ case when the asymmetry of the response functions needs to be included. This will allow a more realistic modelling of sp-valent systems such as carbon and silicon.

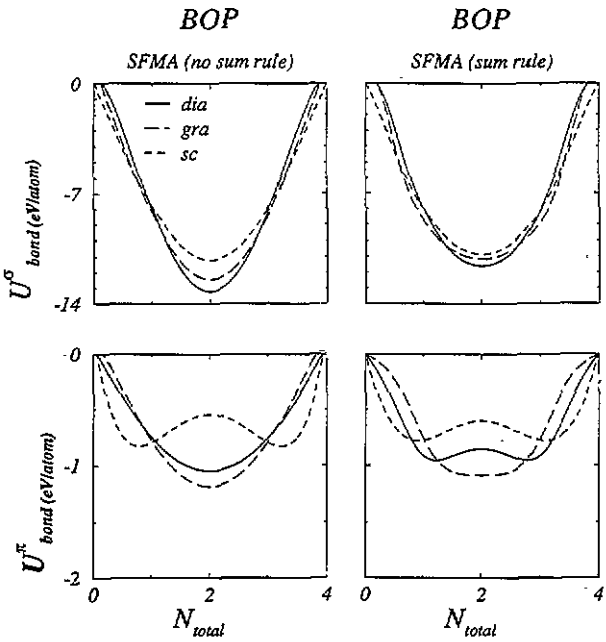

Figure 9. The σ and π bond energy as a function of the total number of electrons per atom within the SFMA when the sum rule is not applied (the left-hand panels) and when it is satisfied (the right-hand panels).

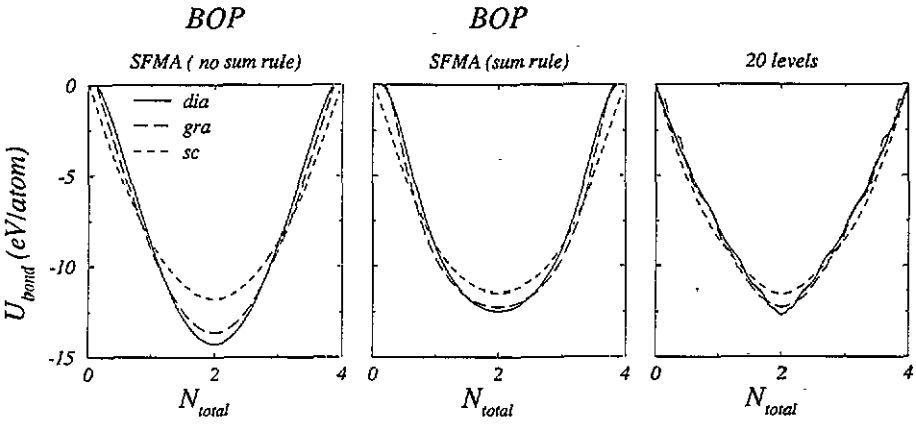

Figure 10. The relative structural trend between sp-valent diamond, graphite and simple cubic lattices within the SFMA when the sum rule is not applied (the left-hand panel), when it is satisfied (the middle panel) and within the intersite method calculated with 20 exact levels around a given bond (the right-hand panel).

Acknowledgments

PG would like to thank the SERC for financial support. We would like to thank Dr Masato Aoki very much for helpful discussions and for making available his analytic expressions for the response functions.

Appendix

Aoki (1991) has derived analytic expressions for the response functions. Within the SFMA χ_2 and χ_4 are given by

$$\chi_2(\varepsilon_F) = \left(\beta_1^2\beta_2^2/32b_\infty\pi\right)\left[\tfrac{1}{4}(1-\beta_2^2)v_3(\varepsilon_F) + \tfrac{1}{16}(\beta_1^2\beta_2^2/2 - \beta_1^2 + \beta_2^4)v_1(\varepsilon_F)\right] \tag{53}$$

$$\chi_4(\varepsilon_F) = \left(\beta_1^2\beta_2^2/32b_\infty\pi\right)\left[\tfrac{1}{4}(1-\beta_2^2/2)v_3(\varepsilon_F) - \left(\beta_1^2/16\right)v_1(\varepsilon_F)\right] \tag{54}$$

where $\varepsilon = E/2b_\infty$ and $\beta_n = b_n^0/b_\infty$ and the recursion coefficients b_n have been chosen to be negative. The number of valence electrons per spin per atom, $N(\leq 1)$, is in the form

$$N = \frac{-\beta_1^2\beta_2^2}{16\pi}u_0(\varepsilon_F) \tag{55}$$

where

$$v_n(\varepsilon_F) = \int_1^{\varepsilon_F} \frac{\varepsilon^n\sqrt{1-\varepsilon^2}}{f_2^2(\varepsilon)}\,\mathrm{d}\varepsilon \tag{56}$$

$$u_0(\varepsilon_F) = \int_1^{\varepsilon_F} \frac{\sqrt{1-\varepsilon^2}}{f_2(\varepsilon)}\mathrm{d}\varepsilon \tag{57}$$

with

$$f_2(\varepsilon) = \left(\varepsilon^4/4\right)(1-\beta_2^2) + \left(\varepsilon^2/16\right)\left(\beta_2^4 + \beta_1^2\beta_2^2 - 2\beta_1^2\right) + \left(\beta_1^4/64\right) \tag{58}$$

References

Aoki M 1991 *private communication*

—— 1993 private communication

Aoki M and Pettifor D G 1993 *Physics of Transition Metals* ed P M Oppeneer and J Kübler (Singapore: World Scientific) p 299

Aoki M, Gumbsch P and Pettifor D G 1993a *Proc. of 15th Taniguchi Symp.* to be published in *Springer Proc. Phys.*

—— 1993b *Proc. 2nd Int. Conf. on Computer Applications to Materials and Molecular Science and Engineering—CAMSE* ed M Doyama (Amsterdam: Elsevier) to be published

Baskes M I, Nelson J S and Wright A F 1989 *Phys. Rev.* B **40** 6085

Brown R H and Carlsson A E 1985 *Phys. Rev.* B **32** 6125

Chadi D J 1979 *J. Vac. Sci. Technol.* **16** 1290

Cressoni J C and Pettifor D G 1991 *J. Phys.: Condens. Matter* **3** 495

Daw M S and Baskes M I 1984 *Phys. Rev.* B **29** 6443

Daw M S and Schlüter M A (ed) 1990 *Atomic Scale Calculations of Structure in Material* (Pittsburgh, PA: Materials Research Society)

Finnis M W, Paxton T, Pettifor D G, Sutton A P and Ohta Y 1988 *Phil. Mag.* A **58** 143

Finnis M W and Sinclair J E 1984 *Phil. Mag.* A **50** 45

Haydock R 1980 *Solid State Physics* vol 35 (New York: Academic) p 216

Haydock R, Heine V and Kelly M J 1972 *J. Phys. C: Solid State Phys.* **5** 2845

Pettifor D G 1986 *J. Phys. C: Solid State Phys.* **19** 285

—— 1989 *Phys. Rev. Lett.* **63** 2480

—— 1990 *Springer Proc. Phys.* **48** 64

Pettifor D G and Aoki M 1991 *Phil. Trans. Royal Soc. (London)* A **334** 439

—— 1992 *Structure and Phase Stability of Alloys* ed J L Moran-Lopez, F Mejia-lira and J M Sanchez (New York: Plenum) p 119

Pettifor D G and Podloucky R 1984 *Phys. Rev. Lett.* **53** 1080

Slater J C and Koster G F 1954 *Phys. Rev.* **94** 1498

Stillinger F H and Weber T A 1985 *Phys. Rev.* B **31** 5262

Sutton A P, Finnis M W, Pettifor D G and Ohta Y 1988 *J. Phys. C: Solid State Phys.* **21** 35

Tersoff J 1988 *Phys. Rev.* B **38** 9902

Turchi P, Ducastelle F and Treglia G 1982 *J. Phys. C: Solid State Phys.* **15** 2891

Vitek V and Srolovitz D J (ed) 1989 *Atomistic Simulation of Materials* (New York: Plenum)